

A Facile Approach toward Multicomponent Supramolecular Structures: Selective Self-Assembly via Charge Separation

Yao-Rong Zheng,* Zhigang Zhao, Ming Wang, Koushik Ghosh, J. Bryant Pollock, Timothy R. Cook, and Peter J. Stang*

Department of Chemistry, University of Utah, 315 South 1400 East, Room 2020, Salt Lake City, Utah 84112, United States

Received July 14, 2010; E-mail: zheng@chem.utah.edu; stang@chem.utah.edu

Abstract: A novel approach toward the construction of multicomponent two-dimensional (2-D) and three-dimensional (3-D) metallosupramolecules is reported. Simply by mixing carboxylate and pyridyl ligands with *cis*-Pt(PET₃)₂(OTf)₂ in a proper ratio, coordination-driven self-assembly occurs, allowing for the selective generation of discrete multicomponent structures via charge separation on the metal centers. Using this method, a variety of 2-D rectangles and 3-D prisms were prepared under mild conditions. Moreover, multicomponent self-assembly can also be achieved by supramolecule-to-supramolecule transformations. The products were characterized by ³¹P and ¹H multinuclear NMR spectroscopy, electrospray ionization mass spectrometry, and pulsed-field-gradient spin echo NMR techniques together with computational simulations.

Introduction

Over the past decade, coordination-driven self-assembly has evolved into a well-established methodology for constructing novel metallosupramolecular structures using dative metal–ligand bonding interactions. A variety of elaborate metallosupramolecules, from two-dimensional (2-D) polygons to three-dimensional (3-D) cages, prisms, and polyhedra, have been reported based on coordination-driven self-assembly.¹ By virtue of the resulting well-defined structures, coordination-driven self-assembly has a wide range of applications, such as synthesis of metallosupramolecular dendrimers,² encapsulation of guests,³ and uses in catalysis⁴ and sensors.⁵ However, the design of coordination-driven self-assembly has been mostly constrained

to two-component systems, in which only one metallic component and one organic component are used.¹ The two-component approach endows coordination-driven self-assembly with easy control and design, but it significantly limits the versatility of molecular components involved and, therefore, the diversity of the resulting supramolecules.⁶ In order to broaden the diversity of coordination-driven self-assembly, it is essential to explore controlled self-assembly within a multicomponent system.

Multicomponent, selective self-assembly represents a unique assembly process in which multiple, varying components can selectively recognize and combine to generate only one discrete structure within a mixture.⁷ Multicomponent, selective self-assembly is a critical phenomenon in many biological systems. Viral capsids such as tomato bushy stunt virus and rhinovirus,

- (1) (a) Stang, P. J.; Olenyuk, B. *Acc. Chem. Res.* **1997**, *30*, 502. (b) Leininger, S.; Olenyuk, B.; Stang, P. J. *Chem. Rev.* **2000**, *100*, 853. (c) Holliday, B. J.; Mirkin, C. A. *Angew. Chem., Int. Ed.* **2001**, *40*, 2022. (d) Fujita, M.; Umemoto, K.; Yoshizawa, M.; Fujita, N.; Kusukawa, T.; Biradha, K. *Chem. Commun.* **2001**, 509. (e) Seidel, S. R.; Stang, P. J. *Acc. Chem. Res.* **2002**, *35*, 972. (f) Ruben, M.; Rojo, J.; Romero-Salguero, F. J.; Uppadine, L. H.; Lehn, J.-M. *Angew. Chem., Int. Ed.* **2004**, *43*, 3644. (g) Fiedler, D.; Leung, D. H.; Bergman, R. G.; Raymond, K. N. *Acc. Chem. Res.* **2005**, *38*, 351. (h) Fujita, M.; Tominaga, M.; Hori, A.; Therrien, B. *Acc. Chem. Res.* **2005**, *38*, 369. (i) Lukin, O.; Voegtli, F. *Angew. Chem., Int. Ed.* **2005**, *44*, 1456. (j) Severin, K. *Chem. Commun.* **2006**, 3859. (k) Nitschke, J. R. *Acc. Chem. Res.* **2007**, *40*, 103. (l) Pitt, M. A.; Johnson, D. W. *Chem. Soc. Rev.* **2007**, *36*, 1441. (m) Oliver, C. G.; Ulman, P. A.; Wiester, M. J.; Mirkin, C. A. *Acc. Chem. Res.* **2008**, *41*, 1618. (n) Parkash, M. J.; Lah, M. S. *Chem. Commun.* **2009**, 3326.
- (2) (a) Yang, H.-B.; Das, N.; Huang, F.; Hawkrigide, A. M.; Muddiman, D. C.; Stang, P. J. *J. Am. Chem. Soc.* **2006**, *128*, 10014. (b) Yang, H.-B.; Hawkrigide, A. M.; Huang, S. D.; Das, N.; Bunge, S. D.; Muddiman, D. C.; Stang, P. J. *J. Am. Chem. Soc.* **2007**, *129*, 2120. (c) Baytekin, H. T.; Sahre, M.; Rang, A.; Engeser, M.; Schulz, A.; Schalley, C. A. *Small* **2008**, *4*, 1823. (d) Yang, H.-B.; Northrop, B. H.; Zheng, Y.-R.; Ghosh, K.; Lyndon, M. M.; Muddiman, D. C.; Stang, P. J. *J. Org. Chem.* **2009**, *74*, 3524. (e) Yang, H.-B.; Northrop, B. H.; Zheng, Y.-R.; Ghosh, K.; Stang, P. J. *J. Org. Chem.* **2009**, *74*, 7067. (f) Zheng, Y.-R.; Ghosh, K.; Yang, H.-B.; Stang, P. J. *Inorg. Chem.* **2010**, *49*, 4747.
- (3) (a) Pluth, M. D.; Bergman, R. G.; Raymond, K. N. *J. Am. Chem. Soc.* **2008**, *130*, 6362. (b) Klosterman, J. K.; Yamauchi, Y.; Fujita, M. *Chem. Soc. Rev.* **2009**, *38*, 1714. (c) Yamauchi, Y.; Yoshizawa, M.; Akita, M.; Fujita, M. *Proc. Natl. Acad. Sci. U.S.A.* **2009**, *106*, 10435. (d) Hatakeyama, Y.; Sawada, T.; Kawano, M.; Fujita, M. *Angew. Chem., Int. Ed.* **2009**, *48*, 8695. (e) Pluth, M. D.; Fiedler, D.; Mugridge, J. S.; Bergman, R. G.; Raymond, K. N. *Proc. Natl. Acad. Sci. U.S.A.* **2009**, *106*, 10438. (f) Mal, P.; Breiner, B.; Rissanen, K.; Nitschke, J. R. *Science* **2009**, *324*, 1697. (g) Sawada, T.; Fujita, M. *J. Am. Chem. Soc.* **2010**, *132*, 7194.
- (4) (a) Yoshizawa, M.; Tamura, M.; Fujita, M. *Science* **2006**, *312*, 251. (b) Pluth, M. D.; Bergman, R. G.; Raymond, K. N. *Science* **2007**, *316*, 85. (c) Pluth, M. D.; Bergman, R. G.; Raymond, K. N. *Acc. Chem. Res.* **2009**, *42*, 1650. (d) Yoshizawa, M.; Klosterman, J. K.; Fujita, M. *Angew. Chem., Int. Ed.* **2009**, *48*, 3418.
- (5) (a) Yamashita, K.-I.; Kawano, M.; Fujita, M. *Chem. Commun.* **2007**, *40*, 4102. (b) Lee, S. J.; Lin, W. *Acc. Chem. Res.* **2008**, *41*, 521. (c) Steed, J. W. *Chem. Soc. Rev.* **2009**, *38*, 506. (d) Liu, Y.; Wu, X.; He, C.; Jiao, Y.; Duan, C. *Chem. Commun.* **2009**, *48*, 7554.
- (6) De, S.; Mahata, K.; Schmittel, M. *Chem. Soc. Rev.* **2010**, *39*, 1555.
- (7) (a) Lehn, J.-M. *Science* **2002**, *295*, 2400. (b) Lehn, J.-M. *Rep. Prog. Phys.* **2004**, *67*–249. (c) Lehn, J.-M. *Chem. Soc. Rev.* **2008**, *36*, 151.

for example, are assembled by three and four different subunits.⁸ The proteasome of yeast *Saccharomyces cerevisiae* is constructed from pairs of seven different proteins.⁹ However, obtaining multicomponent, selective self-assembly in an abiological system is a formidable challenge. By mixing various molecular components that lack sufficient complementary electronic and/or structural information, a self-organized mixture or even disordered oligomeric species can be formed instead of one finite, discrete supramolecule.¹⁰ How to provide sufficient molecular information to control selective self-assembly in a multicomponent system remains a demanding issue in modern supramolecular chemistry.⁶

In the area of coordination-driven self-assembly, several methods have been developed to achieve multicomponent, selective self-assembly. Sauvage¹¹ and Lehn,¹² in pioneering studies, used topological information to guide the selective self-assembly of multicomponent pseudorotaxanes. Recently, it was found that steric constraint could be exploited to control multicomponent, selective self-assembly, as evidenced by the impressive examples of Schmittel,¹³ Fujita,¹⁴ and Kobayashi.¹⁵ However, the incorporation of topological or steric information into molecular components requires significant synthetic effort. Fujita demonstrated the facile, selective self-assembly of 3-D trigonal prisms by mixing palladium(II) acceptors with di- and triopic pyridyl ligands, but a template was essential for the self-assembly.¹⁶

Recently, we demonstrated the facile selective self-assembly of multicomponent 2-D fused polygons and 3-D tetragonal

prisms,¹⁷ and both were achieved just by mixing suitable directional organoplatinum acceptors and different pyridyl donors without templates. These assemblies rely mainly on the stoichiometry and directionality of their molecular components and are controlled by maximum site occupancy and entropy. To further extend the scope of facile, selective self-assembly and the diversity of multicomponent coordination-driven self-assembly, herein we present a multicomponent approach using the coordination-driven self-assembly of a 90° Pt(II) acceptor with pyridyl and carboxylate ligands. With suitable stoichiometry and geometries of the molecular binding units, 2-D supramolecular rectangles (Scheme 1) and 3-D prisms (Scheme 2) can be obtained selectively from multicomponent mixtures, due to the lower energy of the heteroleptic system relative to other products, as shown in Scheme 3. The products were characterized via ³¹P and ¹H multinuclear NMR spectroscopy, electrospray ionization (ESI) mass spectrometry, and pulsed-field-gradient spin-echo (PGSE) NMR measurements together with computational simulations. In addition, a porphyrin tetragonal prism constructed by this method demonstrated the ability to encapsulate triphenylene in an aqueous acetone solution.

Furthermore, this selective self-assembly can be achieved not only by the assembly of the individual molecular components but also via supramolecule-to-supramolecule transformations. Supramolecular transformations have been reported that rely on triggering of the molecular subunits by light, solvent variation, or chemical signals,¹⁸ but this phenomenon is rarely observed in a selective self-assembly system.¹⁹ We investigated supramolecular transformations in multicomponent, selective self-assembly as shown in Scheme 4, where 90° Pt(II) acceptors and pyridyl ligands self-assemble into well-defined homoleptic⁶ supramolecular structures. Addition of a neutral triangle, assembled from the 90° Pt(II) acceptor and a carboxylate ligand, to the pyridyl-based square results in conversion of the homoleptic structures into a single, multicomponent heteroleptic⁶ supramolecule of different topology. These supramolecular transformation processes may be monitored by ³¹P and ¹H multinuclear NMR spectroscopy.

Results and Discussions

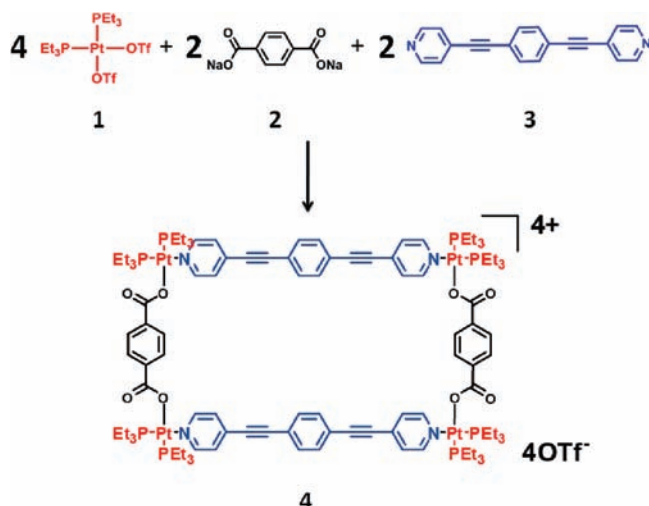
Selective Self-Assembly of a Multicomponent Supramolecular Rectangle. *cis*-Pt(PET₃)₂(OTf)₂ (**1**) was mixed with dicarboxylate ligand **2** and linear dipyridyl donor **3** in a 2:1:1 ratio, followed by addition of D₂O and acetone-*d*₆. After 3 h of heating at 75 °C, all solvent was removed from the clear solution, and acetone-*d*₆ was then added into the mixture. A clear solution was afforded after an additional 5 h of heating at 75 °C, containing the supramolecular rectangle **4** as shown in Scheme 1. ³¹P and ¹H multinuclear NMR spectroscopy and ESI mass spectrometry were used to characterize **4**.

In the ³¹P{¹H} NMR spectrum (Figure 1b), two coupled doublets at 6.60 and 1.06 ppm (²J_{P-P} = 22.0 Hz) of approximately equal intensity with concomitant ¹⁹⁵Pt satellites were

- (8) (a) Abad-Zapatero, C.; Abdel-Meguid, S. S.; Johnson, J. E.; Leslie, A. G. W.; Rayment, I.; Rossmann, M. G.; Suck, D.; Tsukihara, T. *Nature* **1980**, *286*, 33. (b) Rossmann, M. G.; Arnold, E.; Erickson, J. W.; Frankenberger, E. A.; Griffith, J. P.; Hecht, H. J.; Johnson, J. E.; Kamer, G.; Luo, M.; Mosser, A. G.; Rueckert, R. R.; Sherry, B.; Vriend, G. *Nature* **1985**, *317*, 145.
- (9) Groll, M.; Ditzel, L.; Lowe, J.; Stock, D.; Bochter, M.; Bartunik, H. D.; Huber, R. *Nature* **1997**, *386*, 463.
- (10) (a) Zheng, Y.-R.; Yang, H.-B.; Northrop, B. H.; Ghosh, K.; Stang, P. J. *Inorg. Chem.* **2008**, *47*, 4706. (b) Northrop, B. H.; Yang, H.-B.; Stang, P. J. *Inorg. Chem.* **2008**, *47*, 11257. (c) Northrop, B. H.; Zheng, Y.-R.; Chi, K.-W.; Stang, P. J. *Acc. Chem. Res.* **2009**, *42*, 1554. (d) Zheng, Y.-R.; Yang, H.-B.; Ghosh, K.; Zhao, L.; Stang, P. J. *Chem. Eur. J.* **2009**, *15*, 7203.
- (11) (a) Sauvage, J.-P.; Weiss, J. *J. Am. Chem. Soc.* **1985**, *107*, 6108. (b) Nierengarten, J. F.; Dietrich-Buchecker, C. O.; Sauvage, J.-P. *J. Am. Chem. Soc.* **1994**, *116*, 375. (c) Amabilino, D. A.; Dietrich-Buchecker, C. O.; Sauvage, J.-P. *J. Am. Chem. Soc.* **1996**, *118*, 3285. (d) Solladié, N.; Chambron, J.-C.; Sauvage, J.-P. *J. Am. Chem. Soc.* **1999**, *121*, 3684.
- (12) Sleiman, H.; Baxter, P.; Lehn, J.-M.; Rissanen, K. *J. Chem. Soc., Chem. Commun.* **1995**, 715.
- (13) (a) Schmittel, M.; Ganz, A. *Chem. Commun.* **1997**, 999. (b) Schmittel, M.; Ganz, A.; Fenske, D. *Org. Lett.* **2002**, *4*, 2289. (c) Schmittel, M.; Ammon, H.; Kalsani, V.; Wiegrefe, A.; Michel, C. *Chem. Commun.* **2002**, 2566. (d) Schmittel, M.; Kalsani, V.; Fenske, D.; Wiegrefe, A. *Chem. Commun.* **2004**, *5*, 490. (e) Schmittel, M.; Kalsani, V.; Bats, J. W. *Inorg. Chem.* **2005**, *44*, 4115. (f) Schmittel, M.; Mahata, K. *Angew. Chem., Int. Ed.* **2008**, *47*, 5284. (g) Schmittel, M.; Mahata, K. *Inorg. Chem.* **2009**, *48*, 822. (h) Fan, J.; Bats, J. W.; Schmittel, M. *Inorg. Chem.* **2009**, *48*, 6338. (i) Mahata, K.; Schmittel, M. *J. Am. Chem. Soc.* **2009**, *131*, 16544.
- (14) (a) Yoshizawa, M.; Nagao, M.; Kumazawa, K.; Fujita, M. *J. Organomet. Chem.* **2005**, *690*, 5383. (b) Yamauchi, Y.; Fujita, M. *Chem. Commun.* **2010**, *46*, 5897.
- (15) Yamanaka, M.; Yamada, Y.; Sei, Y.; Yamaguchi, K.; Kobayashi, K. *J. Am. Chem. Soc.* **2006**, *128*, 1531.
- (16) (a) Kumazawa, K.; Biradha, K.; Kusukawa, T.; Okano, T.; Fujita, M. *Angew. Chem., Int. Ed.* **2003**, *42*, 3909. (b) Yoshizawa, M.; Nakagawa, J.; Kumazawa, K.; Nagao, M.; Kawano, M.; Ozeki, T.; Fujita, M. *Angew. Chem., Int. Ed.* **2005**, *44*, 1810.

- (17) (a) Lee, J.; Ghosh, K.; Stang, P. J. *J. Am. Chem. Soc.* **2009**, *131*, 12028. (b) Wang, M.; Zheng, Y.-R.; Ghosh, K.; Stang, P. J. *J. Am. Chem. Soc.* **2010**, *132*, 6282.
- (18) (a) Sun, S.-S.; Anspach, J. A.; Lees, A. J. *Inorg. Chem.* **2002**, *41*, 1862. (b) Sun, S.-S.; Stern, C. L.; Nguyen, S. T.; Hupp, J. T. *J. Am. Chem. Soc.* **2004**, *126*, 6314. (c) Heo, J.; Jeon, Y.-M.; Mirkin, C. A. *J. Am. Chem. Soc.* **2007**, *129*, 7712. (d) Zhao, L.; Northrop, B. H.; Stang, P. J. *J. Am. Chem. Soc.* **2008**, *130*, 11886.
- (19) Campbell, V. E.; Hatten, X.; Delsuc, N.; Kauffmann, B.; Huc, I.; Nitschke, J. R. *Nature Chem.* **2010**, *2*, 684.

Scheme 1. Selective Self-Assembly of a Multicomponent Rectangle (**4**) by the Combination of *cis*-Pt(PEt₃)₂(OTf)₂ (**1**), Dicarboxylate Ligand **2**, and Linear Dipyridyl Donor **3**



found, indicating that the Pt(II) centers of **4** bear a heteroleptic coordination motif with pyridyl and carboxylate moieties.²⁰ The doublet at 1.06 ppm is shifted approximately 12 ppm upfield relative to that for **1** (Figure 1a) upon coordination and corresponds to the phosphorus nuclei *trans* to the pyridine ring, while the doublet at 6.60 ppm is due to the phosphorus nuclei opposite to the carboxylate group.^{20a-c} The two signals are coupled, indicating that chemically inequivalent phosphorus nuclei are bound to the same Pt(II) center, consistent with the heteroleptic coordination motif of rectangle **4**. In the ¹H NMR spectrum (Figure S1 in the Supporting Information), signals

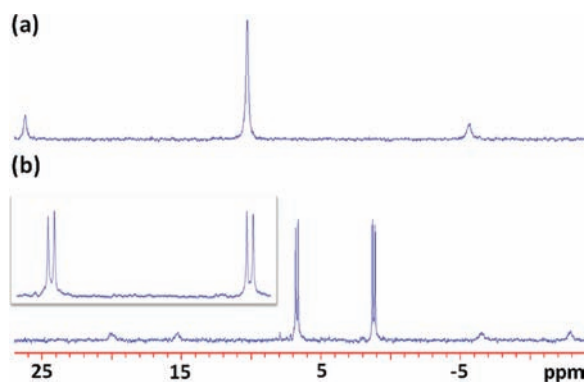


Figure 1. ³¹P{¹H} NMR spectra of *cis*-Pt(PEt₃)₂(OTf)₂ **1** (a) and the multicomponent supramolecular rectangle **4** (b).

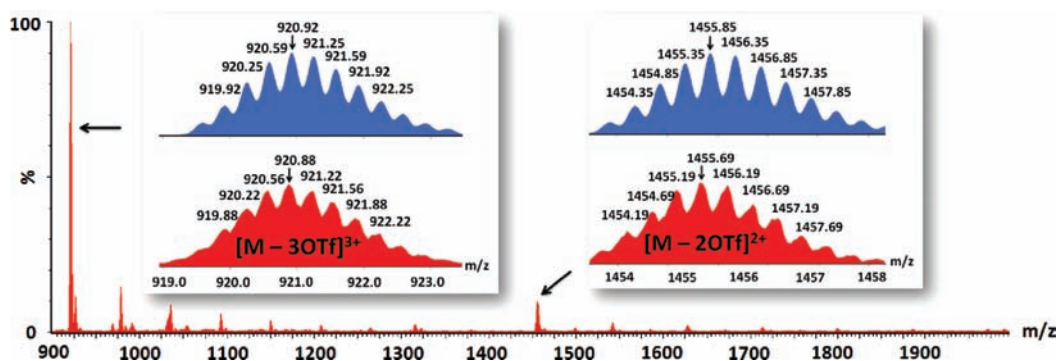


Figure 2. Full ESI mass spectrum of the solution of the multicomponent supramolecular rectangle **4**.

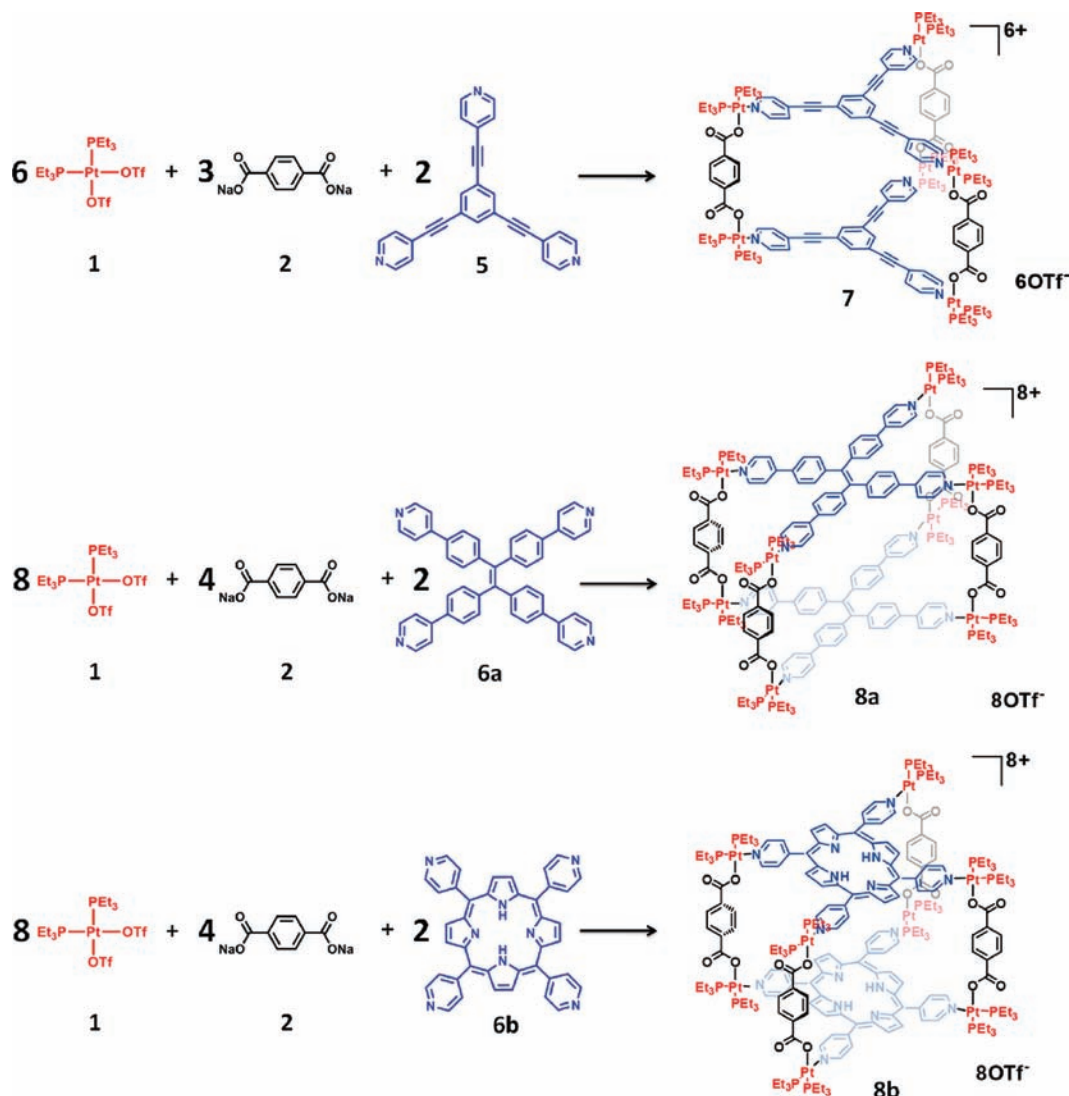
corresponding to the coordinated pyridine and carboxylate ligands were identified at 9.00 (H_{α-Py}), 7.74 (H_{β-Py}), and 7.66 ppm (H_{phenyl}). The sharp and identifiable signals in both the ³¹P{¹H} and ¹H NMR spectra support the self-assembly of the highly symmetric rectangle **4** as the predominant product in the mixture and rule out the formation of homoleptic assemblies or oligomers. ESI mass spectrometry further confirms the formation of a [4+2+2] multicomponent supramolecular rectangle. In Figure 2, peaks attributable to **4** with loss of two and three triflate anions can be observed at *m/z* = 1455.69 ([M - 2OTf]²⁺) and *m/z* = 920.88 ([M - 3OTf]³⁺). All these peaks are isotopically resolved and in good agreement with the theoretical distribution.

Selective Self-Assembly of Multicomponent Supramolecular Prisms. To date, the selective self-assembly of 3-D supramolecules has always required a template¹⁶ and is rarely accomplished based solely on the intrinsic information of the complementary subunits.¹³ Herein, we report the selective self-assembly of 3-D supramolecular prisms by mixing a 90° Pt(II) acceptor, a carboxylate ligand, and different multi-pyridyl ligands, as shown in Scheme 2.

Upon mixing 90° Pt(II) acceptor **1** and carboxylate ligand **2** with tri- or tetrapyridyl donor **5** or **6** in a specific ratio (for **7**, 1:2:5 = 6:3:2; for **8**, 1:2:6 = 8:4:2), supramolecular prisms **7** and **8** were formed as the predominant species after equilibration. The ³¹P{¹H} NMR spectra (Figure 3) of **7** and **8** are dominated by two coupled doublets (**7**, 6.56 and 1.01 ppm, ²J_{P-P} = 22.0 Hz; **8a**, 5.88 and 1.08 ppm, ²J_{P-P} = 21.4 Hz; **8b**, 5.07 and -0.34 ppm, ²J_{P-P} = 21.4 Hz) of similar intensity with concomitant ¹⁹⁵Pt satellites. These data, as expected, support the heteroleptic coordination environments of supramolecular prisms **7** and **8** and rule out the formation of homoleptic complexes or oligomers. Likewise, in the ¹H NMR spectra (Figures S2–S4 in Supporting Information), signals attributable to the coordinated pyridyl and carboxylate moieties are observed: for **7**, 9.02 (H_{α-Py}), 7.75 (H_{β-Py}), and 7.77 ppm (H_{phenyl}); for **8a**, 8.87 (H_{α-Py}), 7.89 (H_{β-Py}), and 7.60 ppm (H_{phenyl}); and for **8b**, 9.27 (H_{α-Py}), 8.34 (H_{β-Py}), and 8.09 ppm (H_{phenyl}). The sharp signals in both the ³¹P{¹H} and ¹H NMR spectra support the predominant formation of highly symmetric supramolecules **7** and **8**.

ESI mass spectral data further support the self-assembly of supramolecular prisms **7** and **8**. As shown in Figure 4 and Figures S5 and S6 in the Supporting Information, intense ESI mass peaks corresponding to consecutive loss of triflate anions from trigonal prism **7** were observed (*m/z* = 2218.76 [M - 2OTf]²⁺ and *m/z* = 1429.59 [M - 3OTf]³⁺), as were those corresponding to the tetragonal prisms **8a** (*m/z* = 2037.75 [M

Scheme 2. Selective Self-Assembly of Multicomponent Trigonal (**7**) and Tetragonal (**8**) Prisms by Combination of *cis*-Pt(PEt₃)₂(OTf)₂ (**1**), Dicarboxylate Ligand **2**, and Tritopic (**5**) and Tetratopic (**6**) Pyridyl Donors



– 3PF₆]³⁺ and $m/z = 1164.50$ [M – 5PF₆]⁶⁺) and **8b** ($m/z = 2022.71$ [M – 3PF₆]³⁺ and $m/z = 1155.62$ [M – 5PF₆]⁵⁺). All of these peaks are isotopically resolved and agree well with their theoretical distributions.

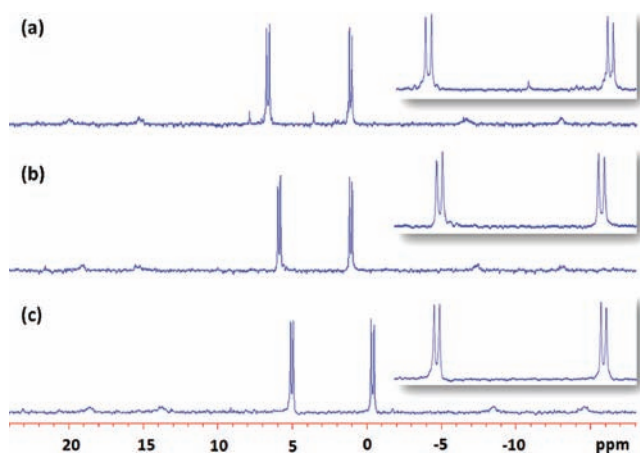


Figure 3. ³¹P{¹H} NMR spectra of the trigonal prism **7** (a) and tetragonal prisms **8a** (b) and **8b** (c).

While suitable X-ray-quality crystals were not obtained, a computational study (see Supporting Information) together with PGSE NMR measurements was carried out to gain insight into the structural parameters of these assemblies.²¹ A molecular dynamics simulation using Maestro and Macromodel with a MMFF or MM2* force field at 300 K in the gas phase was applied to equilibrate each supramolecule, and the output of the simulation was then minimized to full convergence. As shown in Figure 5, models of assemblies **7** and **8** have the shapes of trigonal and tetragonal prisms, respectively, with radii of 12 (**7**), 13 (**8a**), and 12 Å (**8b**). PGSE NMR experiments were carried out to measure the hydrodynamic radius for these assemblies, and the results from these measurements agree with those from the modeled structures: 12.1 ± 0.1 (**7**), 11.6 ± 0.3 (**8a**), and 10.9 ± 0.1 Å (**8b**).

The multinuclear (³¹P and ¹H) NMR spectroscopy, ESI mass spectrometry, and PGSE NMR measurements, along with the computational simulations, clearly support the selective self-assembly of heteroleptic 2-D and 3-D multicomponent supramolecules **4**, **7**, and **8**. To achieve a quantitative insight into such selective multicomponent self-assembly, a computational study was performed to estimate the energy difference between

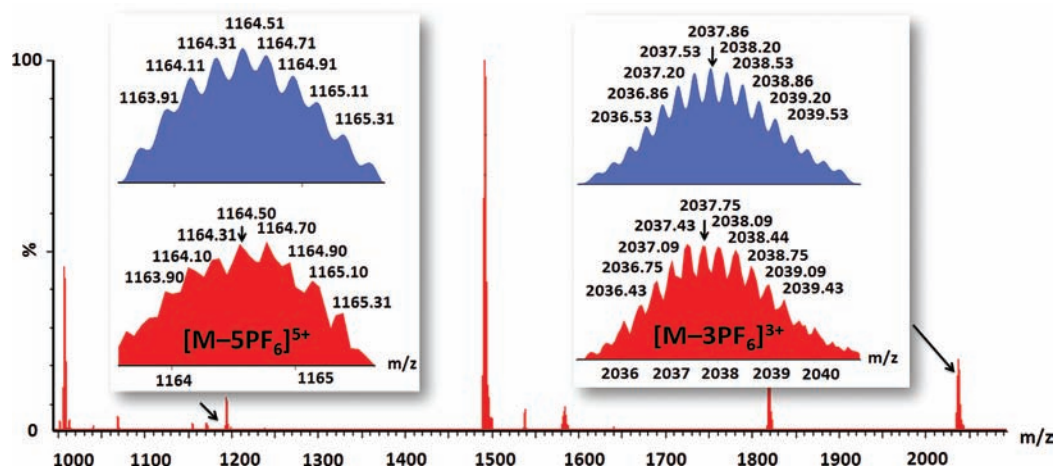


Figure 4. Full ESI mass spectrum of the tetragonal prism 8a.

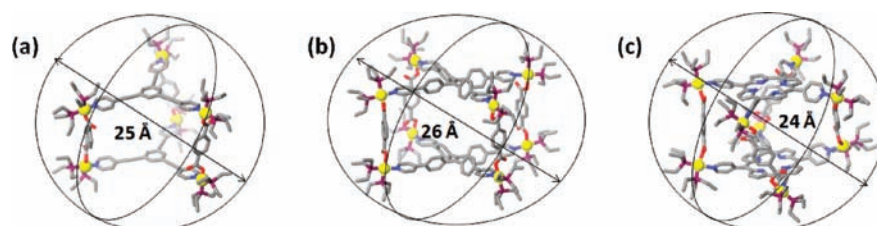
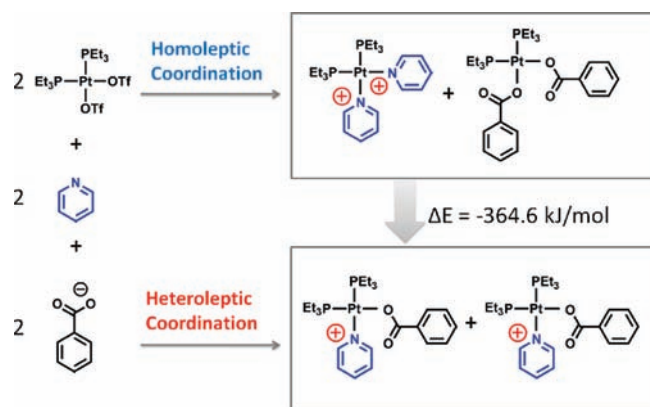


Figure 5. Computational simulations of trigonal prism 7 (a) and tetragonal prisms 8a (b) and 8b (c).

Scheme 3. Representation of Selective Self-Assembly of *cis*-Pt(PEt₃)₂(OTf)₂ with Carboxylate and Pyridyl Moieties Due to the Lower Energy of the Heteroleptic System



the homoleptic and heteroleptic systems. To reduce redundancy and maintain accuracy, a simplified model system was used, as shown in Scheme 3, involving only two 90° acceptors, two pyridines (Py), and two benzoate anions (C₇H₅O₂⁻). Upon heteroleptic coordination (the bottom route in Scheme 3), two heteroleptic molecules of *cis*-Pt(PEt₃)₂PyC₇H₅O₂⁺ may be formed, whereas the top route in Scheme 3 results in the formation of homoleptic species *cis*-Pt(PEt₃)₂Py₂²⁺ and *cis*-Pt(PEt₃)₂(C₇H₅O₂)₂. Computational simulations (MMFF force

field, gas phase, 300 K) for these heteroleptic and homoleptic species were carried out using Maestro and MacroModel. According to MMFF computational results (see Supporting Information), the energy of the system containing two heteroleptic molecules of *cis*-Pt(PEt₃)₂PyC₇H₅O₂⁺ is significantly lower than that with two homoleptic species (ΔE = -364.6 kJ/mol); therefore, the heteroleptic system is favored.

Well supported by both the experimental data and computational calculations, this selective self-assembly is solely driven by the intrinsic information of the molecular components, without involving a template or extra directing factors such as steric and topological constraints.^{13–15} Presumably, the different electronic nature of carboxylate (negative) and pyridine (neutral) donors is a major driving factor, which allows for the heteroleptic coordination via charge separation. For example, in the simplified system illustrated in Scheme 3, within the homoleptic complex *cis*-Pt(PEt₃)₂Py₂²⁺, two coordinated pyridyl moieties may be partially charged²² and result in electrostatic repulsion between them. On the other hand, for the heteroleptic species *cis*-Pt(PEt₃)₂PyC₇H₅O₂⁺, only one pyridyl moiety is coordinated to each Pt(II) center; therefore, the charges can be separated and the electrostatic repulsion can be reduced. Thus, the heteroleptic complex carries the lower energy. Additional experimental and computational studies are underway to further characterize the preference for heteroleptic complex formation. Understanding the factors driving these systems will allow optimization of this strategy for the formation of new multicomponent assemblies.

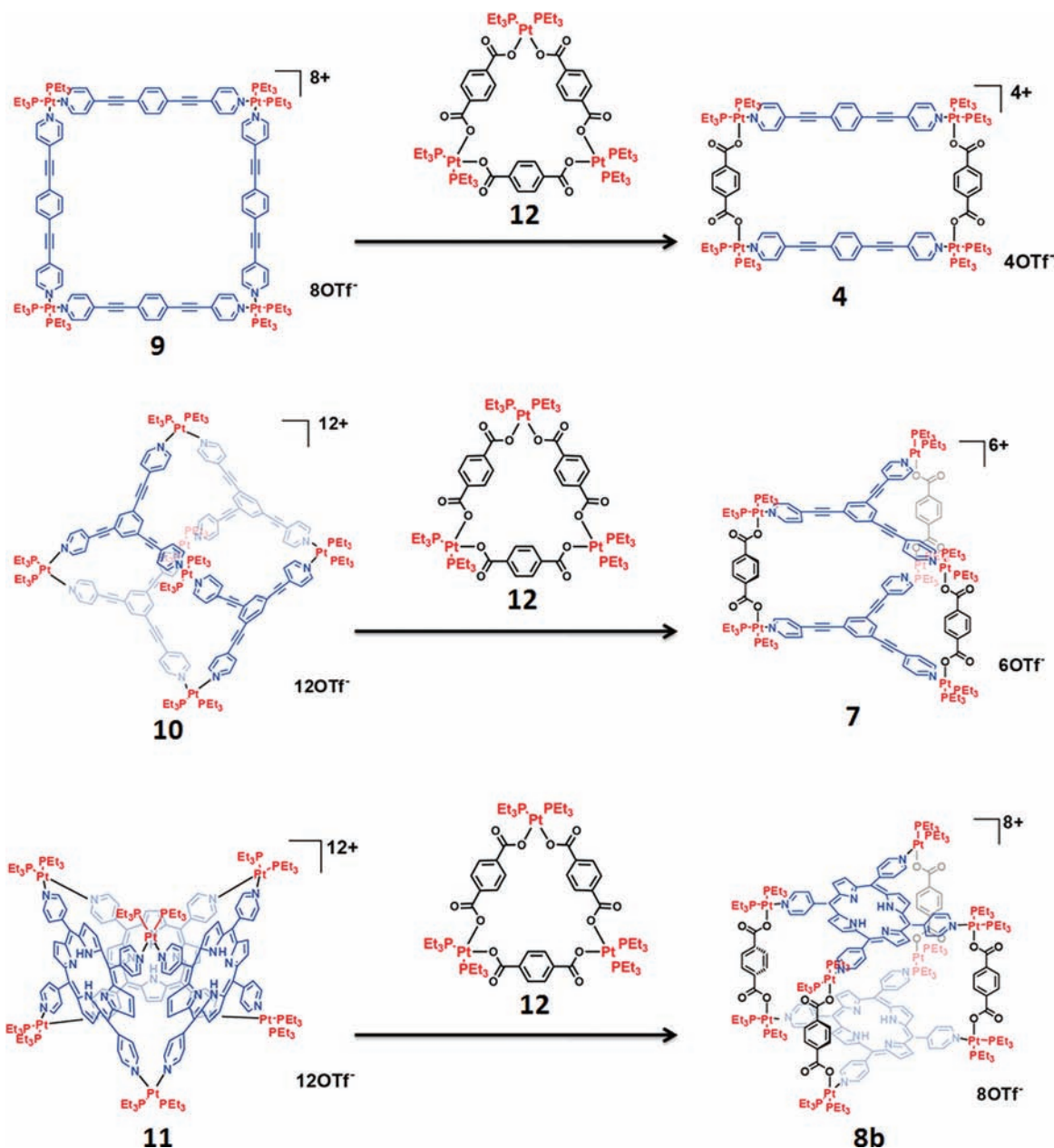
Self-Assembly via Supramolecule-to-Supramolecule Transformations. Multicomponent, selective self-assembly can be achieved not only by the conventional assembly of individual molecular components, as described above, but also via supramolecule-

(20) (a) Chi, K.-W.; Addicott, C.; Arif, A. M.; Stang, P. J. *J. Am. Chem. Soc.* **2004**, *126*, 16569. (b) Chi, K.-W.; Addicott, C.; Kryshchenko, Y. K.; Stang, P. J. *J. Org. Chem.* **2004**, *69*, 964. (c) Chi, K.-W.; Addicott, C.; Moon, M.-E.; Lee, H. J.; Yoon, S. C.; Stang, P. J. *J. Org. Chem.* **2006**, *71*, 6662. (d) Ghosh, S.; Turner, D. R.; Batten, S. R.; Mukherjee, P. S. *Dalton Trans.* **2007**, 1869.

(21) Caskey, D. C.; Yamamoto, T.; Addicott, C.; Shoemaker, R. K.; Vacek, J.; Hawkrige, A. M.; Muddiman, D. C.; Kottas, G. S.; Michl, J.; Stang, P. J. *J. Am. Chem. Soc.* **2008**, *130*, 7620, and references therein.

(22) Penka, E. F.; Schläpfer, C. W.; Atanasov, M.; Albrecht, M.; Daul, C. *J. Organomet. Chem.* **2007**, *692*, 5709.

Scheme 4. Supramolecular Transformations of Square **9**, Truncated Tetrahedron **10**, and Trigonal Prism **11** into Rectangle **4**, Trigonal Prism **7**, and Tetragonal Prism **8b**, Respectively, upon Addition of the Neutral Triangle **12** Assembled by *cis*-Pt(PEt₃)₂(OTf)₂ (**1**) and Carboxylate Ligand **2**



to-supramolecule transformations. Supramolecular transformations may be defined as a process whereby a supramolecular species alters its structure (and composition) upon suitable external stimulus, such as photochemical, electrochemical, or chemical signals.¹⁸ Here, we describe multicomponent, selective self-assembly via supramolecular transformations from homoleptic to heteroleptic systems as shown in Scheme 4. The investigation was carried out by first preparing the homoleptic self-assemblies of 90° Pt(II) acceptor **1** with pyridyl ligands **3**, **4**, and **5b**, and then adding the neutral triangle **12** assembled from 90° Pt(II) acceptor **1** and carboxylate ligand **2**. As a result, the preassembled homoleptic square **9**, truncated tetrahedron **10**, and trigonal prism **11** can be entirely transformed to the multicomponent heteroleptic rectangle **4**, trigonal prism **7**, and tetragonal prism **8b**, respectively.

The homoleptic ensembles **9**, **10**, and **11** as well as the neutral triangle **12** were obtained by mixing the 90° Pt(II) acceptor **1**

with pyridyl ligands **3**, **4**, and **5b** and carboxylate donor **2**, respectively, in 1:1 (**9**), 3:2 (**10**), 2:1 (**11**), and 1:1 (**12**) ratios. Each structure was characterized by ³¹P and ¹H multinuclear NMR spectroscopy, ESI mass spectrometry, and PGSE NMR measurements. In the ³¹P{¹H} NMR spectra (Figure 6a–d), only one intense singlet (**9**, 0.36 ppm; **10**, 0.29 ppm; **11**, 0.90 ppm; **12**, 3.52 ppm) with concomitant ¹⁹⁵Pt satellites can be found. Likewise, the ¹H NMR spectra (Figures S7, S9, S11, and S14 in Supporting Information) show sharp signals assigned to the coordinated pyridyl moieties (e.g., δ = 9.28 ppm, H_{α-Py} in **9**; δ = 9.32 ppm, H_{α-Py} in **10**; δ = 9.75 ppm, H_{α-Py} in **11**) and the carboxylate moieties (δ = 7.74 ppm in **12**). These NMR spectral results are in accord with the highly symmetric structures of **9**–**12**. ESI mass spectrometry further confirms these assemblies (see Supporting Information). Signals for the [4+4] and [6+4] self-assembly of **9** and **10** can be found at *m/z* = 1869.91 [**9** – 2OTf]²⁺, *m/z* = 1197.08 [**9** – 3OTf]³⁺, *m/z* = 1818.36 [**10** –

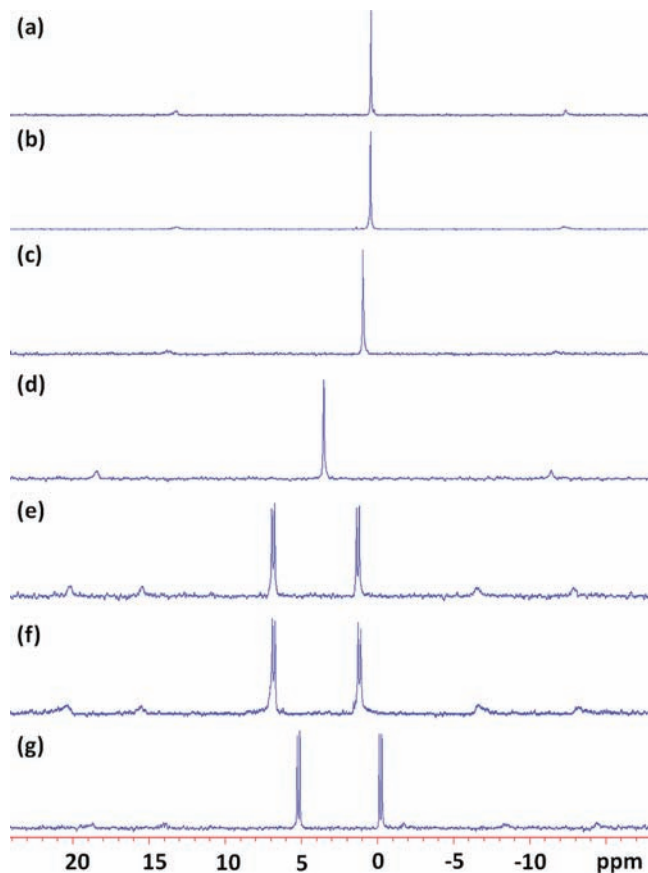


Figure 6. $^{31}\text{P}\{^1\text{H}\}$ NMR spectra of the homoleptic self-assemblies **9** (a), **10** (b), and **11** (c) and the neutral triangle **12** (d), as well as the multicomponent rectangle **4** (e), trigonal prism **7** (f), and tetragonal prism **8b** (g) obtained via supramolecular transformations.

$3\text{OTf}]^{3+}$, and $m/z = 1326.65$ [**10** $-4\text{OTf}]^{4+}$. The [6+3] self-assembly of trigonal prism **11** was also supported by observation of isotopically resolved signals at $m/z = 2966.57$ [**11** $-2\text{OTf}]^{2+}$, $m/z = 1408.99$ [**11** $-4\text{OTf}]^{4+}$, and $m/z = 1097.48$ [**11** $-5\text{OTf}]^{5+}$, but those for larger assemblies such as [4+4], [5+5], and [6+6] could not be found, ruling out the formation of larger prisms.²³ For the neutral triangle **12**, the molecular ion peak for the [3+3] self-assembly was found at $m/z = 1787.12$ [**12** + H]⁺ and $m/z = 1809.11$ [**12** + Na]⁺, along with the signal for [**12** + 2Na]²⁺ at $m/z = 916.16$. There is no molecular ion peak for [2+2] or [4+4] ensembles observed in the mass spectrum, excluding formation of a [2+2] rectangle or a [4+4] square. Furthermore, a PGSE NMR study was also carried out to estimate the size of the trigonal prism **11**, and the experimental radius obtained (1.70 ± 0.04 nm) is in good agreement with the computational value of 1.6 nm from MMFF modeling (Figure S13 in Supporting Information).²¹

The transformation of the homoleptic self-assemblies into the heteroleptic assemblies was carried out by the addition of solutions of the above homoleptic products to the neutral triangle **12**. After 5 h of heating at 75 °C, a clear solution was obtained and characterized by ^{31}P and ^1H multinuclear NMR spectroscopy. In the $^{31}\text{P}\{^1\text{H}\}$ NMR spectra (Figure 6e–g), two intense, coupled doublet peaks (Figure 6e, 6.63 and 1.08 ppm, $^2J_{\text{P-P}} = 22.0$ Hz for **4**; Figure 6f, 6.63 and 1.03 ppm, $^2J_{\text{P-P}} = 21.4$ Hz for **7**; Figure 6g, 5.03 and -0.35 ppm, $^2J_{\text{P-P}} = 21.4$ Hz for **8b**)

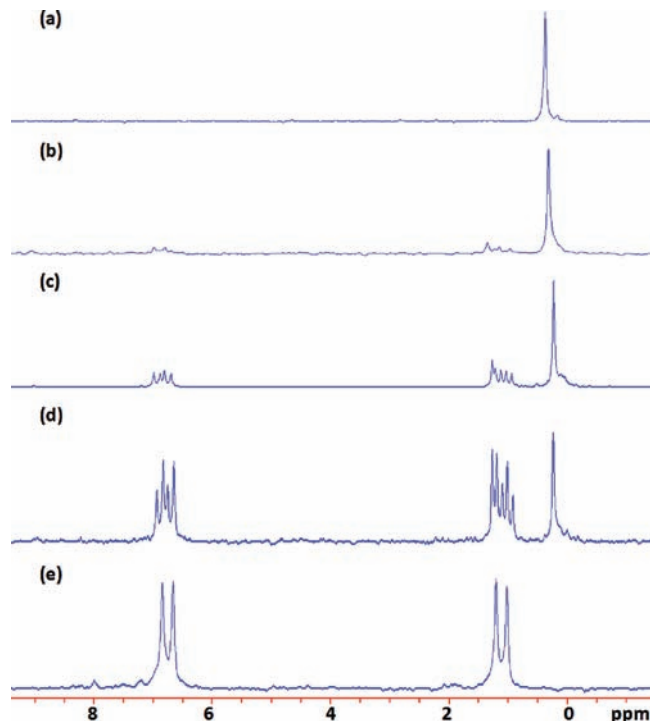


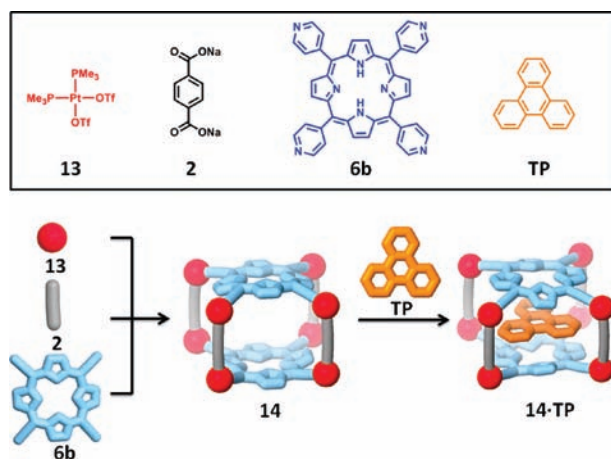
Figure 7. $^{31}\text{P}\{^1\text{H}\}$ NMR spectra for mixtures of square **9** upon addition of 0% (a), 10% (b), 25% (c), 50% (d), and 100% (e) of neutral triangle **12**.

with concomitant ^{195}Pt satellites were found, which were in good agreement with those observed in Figures 1 and 3 for the authentic heteroleptic cages. Likewise, in the ^1H NMR spectra (Figure S16 in Supporting Information), the signals of the heteroleptic structures obtained by supramolecular transformation match the signals of the authentic ensembles. Peaks corresponding to the starting homoleptic structures were absent in both $^{31}\text{P}\{^1\text{H}\}$ and ^1H NMR spectra. These NMR data clearly indicate that the homoleptic assemblies have been entirely transformed into the multicomponent heteroleptic structures.

To further investigate the supramolecular transformation process, we carried out a study of the gradual transformation of square **9** to rectangle **4**: 10%, 25%, 50%, and 100% of neutral triangle **12** was added to an acetone solution of square **9**, and the mixtures were heated at 75 °C for 5 h. The resulting clear solutions were characterized by ^{31}P and ^1H multinuclear NMR spectroscopy. As indicated by the $^{31}\text{P}\{^1\text{H}\}$ NMR spectra (Figure 7), increasing the amount of **12** resulted in a decrease of the signal ($\delta = 0.36$ ppm) for square **9** and the simultaneous formation of signals around 6.63 and 0.99 ppm, attributable to heteroleptic complexes. A similar result was observed in the ^1H NMR spectra (Figure S17 in Supporting Information) by comparing the signals for $\text{H}_{\alpha\text{-Py}}$ of the homoleptic assembly ($\delta = 9.28$ ppm) and the heteroleptic complexes ($\delta = 9.00$ ppm). These ^{31}P and ^1H NMR spectral results demonstrate the gradual transformation of heteroleptic complexes from the homoleptic species upon addition of the neutral triangle. During the transformation process, in addition to rectangle **4**, an intermediate was also observed, indicated by the multiplets around 6.63 and 0.99 ppm in Figure 7b–d. Isotopically resolved signals in the ESI mass spectrum (see Supporting Information) at $m/z = 722.56$ [**M** $-3\text{OTf}]^{3+}$ and $m/z = 1158.25$ [**M** $-2\text{OTf}]^{2+}$ suggest this intermediate is formed by the [3+2+1] assembly of 90° acceptor **1**, pyridyl donor **3**, and carboxylate ligand **2**, and these signals cannot be found in the spectrum of pure rectangle **4**,

(23) Bar, A. K.; Chakrabarty, R.; Mostafa, G.; Mukherjee, P. S. *Angew. Chem., Int. Ed.* **2008**, *47*, 8455.

Scheme 5. Graphical Representation of Self-Assembly of Multicomponent Porphyrin Cage **14** by *cis*-Pt(PMe₃)₂(OTf)₂ (**13**) with Carboxylate **2** and Pyridyl Ligands **6b** and Encapsulation of Triphenylene (TP)



square **9**, or neutral triangle **12**. The intermediate is formed due to the improper ratio of square and neutral triangle for generating the [4+2+2] rectangle **4**. Once 100% of neutral triangle **12** was added, square **9** was fully altered to rectangle **4** as indicated by Figure 7e and Figure S17e.

Host–Guest Properties of the Multicomponent Structure. To explore potential applications of such multicomponent structures, a host–guest study was carried out as shown in Scheme 5: a multicomponent porphyrin cage soluble in aqueous acetone solution was prepared by the method described above and then used as a host for encapsulating the aromatic guest, triphenylene. The multicomponent porphyrin cage **14** was prepared by mixing *cis*-Pt(PMe₃)(OTf)₂ (**13**) with tetrakis(4-pyridyl) porphyrin (**6b**) and sodium terephthalate (**2**) in a 4:1:2 ratio in an aqueous acetone solution (v/v 1:1). After heating at 85 °C for 24 h, a clear, purple solution was obtained. The ³¹P{¹H} NMR spectrum (Figure S19 in the Supporting Information) of the solution shows two doublets at –24.3 and –30.3 ppm of equal intensity, with concomitant ¹⁹⁵Pt satellites. The ¹H NMR spectrum (Figure 8a) shows signals corresponding to coordinated pyridyl and carboxylate moieties, identified at 9.22 (H_{α-Py}), 8.28 (H_{β-Py}), and 7.95

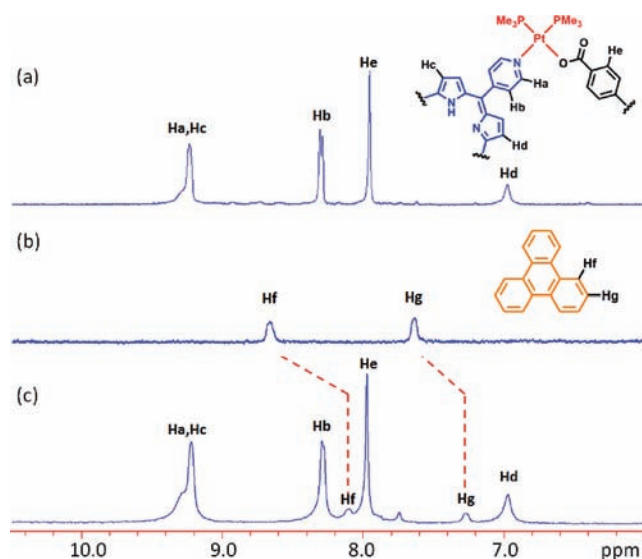


Figure 8. Partial ¹H NMR spectra (300 MHz, acetone-*d*₆/D₂O = 1:1) of pure **14** (a), TP (b), and the host–guest mixture (c).

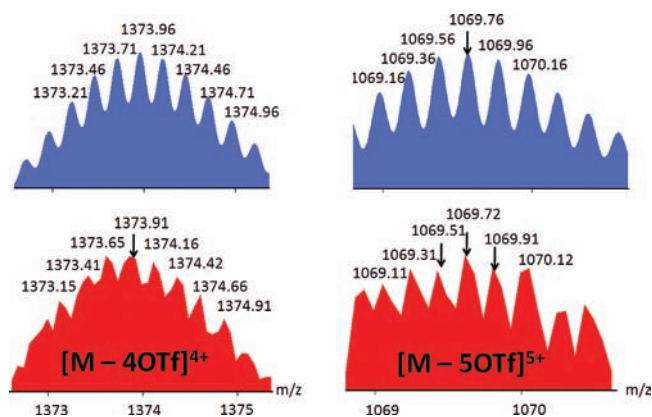


Figure 9. Calculated (blue, top) and experimental (red, bottom) ESI mass spectra of the encapsulated complex **14**·TP.



Figure 10. Varied views of the computational model (MM2*) of the encapsulated complex **14**·TP.

ppm (H_{phenyl-2}). The NMR spectral evidence clearly indicates that a heteroleptic ensemble was predominantly formed in the solution. Isotopically resolved signals in the ESI-MS spectrum at *m/z* = 1806.24 ([**14** – 3OTf]³⁺) and *m/z* = 1317.69 ([**14** – 4OTf]⁴⁺) (Figure S20 in the Supporting Information) further support that the heteroleptic species is the multicomponent porphyrin cage **14**.

The host–guest properties of **14** were studied by the addition of excess triphenylene (TP) in aqueous acetone solution to the cage. After heating at 85 °C for 16 h, the encapsulated complex was present in the mixture. Two doublets at –24.3 and –30.3 ppm with concomitant ¹⁹⁵Pt satellites in the ³¹P{¹H} NMR spectrum (see Supporting Information) and the identifiable peaks (δ = 9.22 ppm for H_{α-Py}, δ = 8.28 ppm for H_{β-Py}, and δ = 7.95 ppm for H_{phenyl-2}) in the ¹H NMR spectrum (Figure 8c) indicated that the coordinative porphyrin cage structure was retained. By comparing the ¹H NMR spectra of pure **14** and TP with the spectrum of the mixture (Figure 8), shifted signals were observed at 8.11 (Δδ = –0.54 ppm, H_{triphenylene}) and 7.26 ppm (Δδ = –0.38 ppm, H_{triphenylene}), indicating that the TP was encapsulated in the porphyrin cage, **14**. The ESI mass spectra (Figure 9) showed isotopically resolved signals at *m/z* = 1373.91 [**14**·TP – 4OTf]⁴⁺ and *m/z* = 1069.72 [**14**·TP – 5OTf]⁵⁺, confirming that one TP molecule was encapsulated in the cage of **14**. Integration of the proton NMR signals indicated that 27% of cage **14** contained guest molecules under these conditions.

A computational simulation was used to gain insight about the structural features of the encapsulated complex **14**·TP. A molecular dynamics simulation using MM2* force fields at 300 K in the aqueous phase was used to equilibrate the complex, and the output of the simulation was then minimized to full convergence. As shown in Figure 10, one TP molecule is

trapped within the cavity of **14**, and the distance between the guest and porphyrin faces is about 3.8 Å.

Conclusion

We report here a facile and very efficient approach for the selective construction of well-defined multicomponent 2-D and 3-D supramolecular structures of various motifs. Upon combination of a 90° Pt(II) acceptor and a carboxylate ligand with appropriate pyridyl donors in a proper ratio, coordination-driven self-assembly allows for the selective formation of multicomponent supramolecular rectangle and prisms. These multicomponent complexes can also be obtained by a novel supramolecule-to-supramolecule transformation from homoleptic assemblies. Characterization via multinuclear (³¹P and ¹H) NMR spectroscopy clearly reveals the heteroleptic coordination nature of these assembled supramolecules, as well as their high structural symmetry. ESI mass spectrometry and PGSE NMR measurements, together with computational simulations, further identify the composition and size of these multicomponent assemblies. Presumably, such multicomponent, selective self-assembly processes are directed, in part, by a charge separation effect, whereby a negative carboxylate ligand and a neutral pyridyl donor favor a heteroleptic motif upon coordination with Pt(II) centers. These cage structures show a unique 3-D nanoscale pore, and preliminary studies indicate that the nanocavity is able to encapsulate triphenylene. These selectively self-assembled multicomponent supramolecules can be further developed into functionalized scaffolds via pre/postmodifications, which is currently under investigation.

Experimental Section

Methods and Materials. Molecular building blocks **1**, **13**,²⁴ **3**,²⁵ **5**,²⁶ and **6a**^{17b} were prepared according to literature procedures. Carboxylate ligand **2** was prepared by neutralization of terephthalic acid with 2 equiv of NaOH. All other reagents were purchased from Aldrich or Alfa and used without further purification. Deuterated solvents were purchased from Cambridge Isotope Laboratory (Andover, MA). Multinuclear (³¹P and ¹H) NMR spectra were recorded on a Varian Unity 300 spectrometer, and PGSE NMR data were obtained on an Inova 500 MHz spectrometer. Mass spectra were recorded on a Micromass Quattro II triple-quadrupole mass spectrometer using electrospray ionization with a MassLynx operating system. Element analysis was performed by Atlantic Microlab (Norcross, GA).

General Procedure for Selective Self-Assembly. *cis*-Pt(PEt₃)₂(OTf)₂ (**1**), carboxylate ligand **2**, and various pyridyl donors were placed in a 2-dram vial, followed by addition of D₂O (0.2 mL) and acetone-*d*₆ (0.8 mL). After 3 h of heating at 75 °C, all solvent was removed by N₂ flow and then dried under vacuum. Acetone-*d*₆ (0.7 mL) was then added into each mixture. A clear solution was obtained after an additional 5 h of heating at 75 °C. The resulted multicomponent supramolecules were isolated via precipitation by addition of Et₂O or KPF₆.

Synthesis and Characteristics of 4. Reaction scale: *cis*-Pt(PEt₃)₂(OTf)₂ (**1**), 5.37 mg, 7.36 μmol; carboxylate ligand **2**, 0.77 mg, 3.7 μmol; and ditopic pyridyl ligand **3**, 1.03 mg, 3.68 μmol. Yield: 90%. MS (ESI) calcd for [M - 2OTf]²⁺ *m/z* 1455.85, found 1455.69; calcd for [M - 3OTf]³⁺ *m/z* 920.92, found 920.88. ¹H NMR (acetone-*d*₆, 300 MHz) δ 9.00 (s, 8H, H_{α-Py}), 7.74 (m, 16H,

H_{β-Py} and H_{phenyl-Py}), 7.66 (s, 8H, H_{phenyl}), 1.92 (m, 48H, PCH₂CH₃), 1.21 (m, 72H, PCH₂CH₃). ³¹P{¹H} NMR (acetone-*d*₆, 121.4 MHz) δ 6.60 (d, ²J_{P-P} = 22.0 Hz, ¹⁹⁵Pt satellites, ¹J_{Pt-P} = 3242 Hz), 1.06 (d, ²J_{P-P} = 22.0 Hz, ¹⁹⁵Pt satellites, ¹J_{Pt-P} = 3427 Hz). Anal. Calcd for C₁₀₈H₁₅₂F₁₂N₄O₂₀Pt₈S₄: C, 40.40; H, 4.77; N, 1.74. Found: C, 40.04; H, 4.70; N, 1.71.

Synthesis and Characteristics of 7. Reaction scale: *cis*-Pt(PEt₃)₂(OTf)₂ (**1**), 4.88 mg, 6.69 μmol; carboxylate ligand **2**, 0.71 mg, 3.4 μmol; and tritopic pyridyl ligand **5**, 0.84 mg, 2.2 μmol. Yield: 91%. MS (ESI) calcd for [M - 2OTf]²⁺ *m/z* 2218.98, found 2218.76; calcd for [M - 3OTf]³⁺ *m/z* 1429.67, found 1429.59. ¹H NMR (acetone-*d*₆, 300 MHz) δ 9.02 (s, 12H, H_{α-Py}), 7.88 (s, 12H, H_{phenyl-Py}), 7.75 (m, 24H, H_{β-Py} and H_{phenyl}), 1.89 (m, 72H, PCH₂CH₃), 1.20 (m, 108H, PCH₂CH₃). ³¹P{¹H} NMR (acetone-*d*₆, 121.4 MHz) δ 6.56 (d, ²J_{P-P} = 22.0 Hz, ¹⁹⁵Pt satellites, ¹J_{Pt-P} = 3227 Hz), 1.01 (d, ²J_{P-P} = 22.0 Hz, ¹⁹⁵Pt satellites, ¹J_{Pt-P} = 3404 Hz). Anal. Calcd for C₁₅₆H₂₂₂F₁₈N₆O₃₀Pt₆S₆: C, 39.55; H, 4.72; N, 1.77. Found: C, 39.92; H, 4.54; N, 1.79.

Synthesis and Characteristics of 8a. Reaction scale: *cis*-Pt(PEt₃)₂(OTf)₂ (**1**), 5.22 mg, 7.16 μmol; carboxylate ligand **2**, 0.75 mg, 3.6 μmol; and tetrapic pyridyl ligand **6a**, 1.14 mg, 1.78 μmol. Yield: 96%. MS (ESI) calcd for [M - 3PF₆]³⁺ *m/z* 2037.86, found 2037.75; calcd for [M - 5PF₆]⁵⁺ *m/z* 1164.51, found 1164.50. ¹H NMR (acetone-*d*₆, 300 MHz) δ 8.87 (s, 16H, H_{α-Py}), 7.89 (d, *J* = 6 Hz, 16H, H_{α-phenyl-Py}), 7.60 (m, 32H, H_{β-Py} and H_{phenyl}), 7.20 (d, *J* = 6 Hz, 16H, H_{β-phenyl-Py}), 1.89 (m, 96H, PCH₂CH₃), 1.17 (m, 144H, PCH₂CH₃). ³¹P{¹H} NMR (acetone-*d*₆, 121.4 MHz) δ 5.88 (d, ²J_{P-P} = 21.4 Hz, ¹⁹⁵Pt satellites, ¹J_{Pt-P} = 3270 Hz), 1.08 (d, ²J_{P-P} = 21.4 Hz, ¹⁹⁵Pt satellites, ¹J_{Pt-P} = 3448 Hz). Anal. Calcd for C₂₂₀H₃₂₀F₄₈N₈O₁₆P₂₄Pt₈: C, 40.35; H, 4.93; N, 1.71. Found: C, 40.71; H, 5.08; N, 1.74.

Synthesis and Characteristics of 8b. Reaction scale: *cis*-Pt(PEt₃)₂(OTf)₂ (**1**), 4.52 mg, 6.10 μmol; carboxylate ligand **2**, 0.63 mg, 3.0 μmol; and tetrapic pyridyl ligand **6b**, 0.94 mg, 1.5 μmol. Yield: 95%. MS (ESI) calcd for [M - 3PF₆]³⁺ *m/z* 2022.83, found 2022.71; calcd for [M - 5PF₆]⁵⁺ *m/z* 1155.71, found 1155.62. ¹H NMR (CD₃NO₂, 300 MHz) δ 9.27 (m, 24H, H_{α-Py} and H_{pyrrole}), 8.34 (d, *J* = 5.7 Hz, 16H, H_{β-Py}), 8.08 (s, 16H, H_{phenyl}), 7.12 (s, 8H, H_{pyrrole}), 2.24 (m, 96H, PCH₂CH₃), 1.39 (m, 144H, PCH₂CH₃), -3.28 (s, 4H, H_{N-H}). ³¹P{¹H} NMR (CD₃NO₂, 121.4 MHz) δ 5.07 (d, ²J_{P-P} = 21.4 Hz, ¹⁹⁵Pt satellites, ¹J_{Pt-P} = 3270 Hz), -0.34 (d, ²J_{P-P} = 21.4 Hz, ¹⁹⁵Pt satellites, ¹J_{Pt-P} = 3462 Hz). Anal. Calcd for C₂₀₈H₃₀₈F₄₈N₁₆O₁₆P₂₄Pt₈: C, 38.41; H, 4.77; N, 3.45. Found: C, 38.07; H, 4.92; N, 3.41.

Self-Assembly of 9. *cis*-Pt(PEt₃)₂(OTf)₂ (**1**) (5.07 mg, 6.95 μmol) and ditopic pyridyl ligand **3** (1.95 mg, 6.96 μmol) were placed in a 2-dram vial, followed by addition of 0.7 mL of acetone-*d*₆, and the vial was then sealed with Teflon tape and immersed in an oil bath at 70 °C for 2 h. Solid product was obtained by removing the solvent under vacuum. Yield: 97%. MS (ESI) calcd for [M - 2OTf]²⁺ *m/z* 1869.84, found 1869.91; calcd for [M - 3OTf]³⁺ *m/z* 1197.25, found 1197.08. ¹H NMR (acetone-*d*₆, 300 MHz) δ 9.28 (d, *J* = 4.8 Hz, 16H, H_{α-Py}), 7.79 (d, *J* = 6.0 Hz, 16H, H_{β-Py}), 7.69 (s, 16H, H_{phenyl-Py}), 2.08 (m, 48H, PCH₂CH₃), 1.29 (m, 72H, PCH₂CH₃). ³¹P{¹H} NMR (acetone-*d*₆, 121.4 MHz) δ 0.36 (s, ¹⁹⁵Pt satellites, ¹J_{Pt-P} = 3099 Hz). Anal. Calcd for C₁₃₆H₁₆₈F₂₄N₈O₂₄Pt₄S₈: C, 40.44; H, 4.19; N, 2.77. Found: C, 40.65; H, 4.21; N, 2.64.

Self-Assembly of 10. *cis*-Pt(PEt₃)₂(OTf)₂ (**1**) (4.51 mg, 6.18 μmol) and tritopic pyridyl ligand **5** (1.55 mg, 4.06 μmol) were placed in a 2-dram vial, followed by addition of 0.7 mL of acetone-*d*₆, and the vial was then sealed with Teflon tape and immersed in an oil bath at 70 °C for 2 h. Solid product was obtained by removing the solvent under vacuum. Yield: 98%. MS (ESI) calcd for [M - 3OTf]³⁺ *m/z* 1818.32, found 1818.36; calcd for [M - 4OTf]⁴⁺ *m/z* 1326.75, found 1326.65. ¹H NMR (acetone-*d*₆, 300 MHz) δ 9.32 (d, *J* = 4.8 Hz, 24H, H_{α-Py}), 8.04 (s, 12H, H_{phenyl-Py}), 7.83 (d, *J* = 6.3 Hz, 24H, H_{β-Py}), 2.09 (m, 72H, PCH₂CH₃), 1.29 (m, 108H, PCH₂CH₃). ³¹P{¹H} NMR (acetone-*d*₆, 121.4 MHz) δ 0.29 (s, ¹⁹⁵Pt

(24) Stang, P. J.; Cao, D. H.; Saito, S.; Arif, A. M. *J. Am. Chem. Soc.* **1995**, *117*, 6273.

(25) Kuehl, C. J.; Huang, S. D.; Stang, P. J. *J. Am. Chem. Soc.* **2001**, *123*, 9634.

(26) Lee, S. J.; Mulfort, K. L.; O'Donnell, J. L.; Zuo, X.; Goshe, A. J.; Wesson, P. J.; Nguyen, S. T.; Hupp, J. T.; Tiede, D. M. *Chem. Commun.* **2006**, *44*, 4581.

satellites, $^1J_{\text{Pt-P}} = 3083$ Hz). Anal. Calcd for $\text{C}_{192}\text{H}_{240}\text{F}_{36}\text{N}_{12}\text{O}_{36}\text{P}_{12}\text{Pt}_6\text{S}_{12}$: C, 39.07; H, 4.10; N, 2.85. Found: C, 39.25; H, 4.18; N, 2.81.

Self-Assembly of 11. To a 1.2 mL CD_2Cl_2 suspension of tetratopic pyridyl ligand **6b** (2.46 mg, $3.97 \mu\text{mol}$) was added a 0.4 mL CD_3NO_2 solution of *cis*-Pt(PEt_3) $_2$ (OTf) $_2$ (**1**) (5.89 mg, $8.07 \mu\text{mol}$), drop by drop, with continuous stirring (5 min). The reaction mixture was stirred at room temperature for 1 h and then heated to 70°C overnight. The solution was evaporated to dryness, and the product was collected. Yield: 98%. MS (ESI) calcd for $[\text{M} - 2\text{OTf}]^{2+} m/z$ 2966.54, found 2966.57; calcd for $[\text{M} - 4\text{OTf}]^{4+} m/z$ 1409.04, found 1408.99; calcd for $[\text{M} - 5\text{OTf}]^{5+} m/z$ 1097.44, found 1097.48. ^1H NMR ($\text{CD}_2\text{Cl}_2/\text{CD}_3\text{NO}_2$ 3/1, 300 MHz) δ 9.75 (dd, $J_1 = 4.8$ Hz and $J_2 = 36$ Hz, 24H, $\text{H}_{\alpha\text{-Py}}$), 8.98 (m, 36H, $\text{H}_{\beta\text{-Py}}$ and $\text{H}_{\text{Pyrrole}}$), 8.51 (s, 12H, $\text{H}_{\text{Pyrrole}}$), 2.32 (m, 72H, PCH_2CH_3), 1.60 (m, 108H, PCH_2CH_3). $^{31}\text{P}\{^1\text{H}\}$ NMR ($\text{CD}_2\text{Cl}_2/\text{CD}_3\text{NO}_2$ 3/1, 121.4 MHz) δ 0.90 (s, ^{195}Pt satellites, $^1J_{\text{Pt-P}} = 3070$ Hz). Anal. Calcd for $\text{C}_{204}\text{H}_{258}\text{F}_{36}\text{N}_{24}\text{O}_{36}\text{P}_{12}\text{Pt}_6\text{S}_{12}$: C, 39.31; H, 4.17; N, 5.39. Found: C, 39.83; H, 4.35; N, 5.16.

Self-Assembly of 12. *cis*-Pt(PEt_3) $_2$ (OTf) $_2$ (**1**) (2.12 mg, $2.91 \mu\text{mol}$) and carboxylate ligand **2** (0.61 mg, $2.9 \mu\text{mol}$) were placed in a 2-dram vial, followed by addition of 0.08 mL of H_2O and 0.8 mL of acetone, and the vial was then sealed with Teflon tape and immersed in an oil bath at 70°C for 2 h. The solvent was then removed by N_2 flow. Next, 0.6 mL of acetone- d_6 was added to the dried mixture, and after 4 h of heating at 70°C , the neutral triangle was formed. MS (ESI) calcd for $[\text{M} + \text{H}]^+ m/z$ 1787.38, found 1787.12; calcd for $[\text{M} + \text{Na}]^+ m/z$ 1809.47, found 1809.11; calcd for $[\text{M} + 2\text{Na}]^{2+} m/z$ 916.23, found 916.16. ^1H NMR (acetone- d_6 , 300 MHz) δ 7.74 (s, 12H, H_{phenyl}), 2.00 (m, 36H, PCH_2CH_3), 1.23

(m, 54H, PCH_2CH_3). $^{31}\text{P}\{^1\text{H}\}$ NMR (acetone- d_6 , 121.4 MHz) δ 3.52 (s, ^{195}Pt satellites, $^1J_{\text{Pt-P}} = 3619$ Hz).

Self-Assembly of 14. *cis*-Pt(PMe_3) $_2$ (OTf) $_2$ (**13**) (4.92 mg, $7.63 \mu\text{mol}$), carboxylate ligand **2** (0.81 mg, $3.86 \mu\text{mol}$), and tetratopic pyridyl ligand **6b** (1.20 mg, $1.94 \mu\text{mol}$) were placed in a 2-dram vial, followed by addition of 0.6 mL of D_2O and 0.6 mL of acetone- d_6 , and the vial was then sealed with Teflon tape and immersed in an oil bath at 85°C for 24 h. The multicomponent porphyrin cage **14** was formed. The solid product can be isolated by ion exchange with KPF_6 . Yield: 95%. MS (ESI) calcd for $[\text{M} - 4\text{OTf}]^{4+} m/z$ 1317.69, found 1317.69; calcd for $[\text{M} - 3\text{OTf}]^{3+} m/z$ 1806.23, found 1806.24. ^1H NMR ($\text{D}_2\text{O}/\text{acetone-}d_6$ 1/1, 300 MHz) δ 9.22 (m, 24H, $\text{H}_{\alpha\text{-Py}}$ and $\text{H}_{\text{Pyrrole}}$), 8.28 (d, $J = 5.7$ Hz, 16H, $\text{H}_{\beta\text{-Py}}$), 7.95 (s, 16H, H_{phenyl}), 6.96 (s, 8H, $\text{H}_{\text{Pyrrole}}$), 1.95 (d, $J = 12$ Hz, 72H, PCH_3), 1.80 (d, $J = 12$ Hz, 72H, PCH_3). $^{31}\text{P}\{^1\text{H}\}$ NMR ($\text{D}_2\text{O}/\text{acetone-}d_6$ 1/1, 121.4 MHz) δ -24.3 (d, $^2J_{\text{P-P}} = 23.8$ Hz, ^{195}Pt satellites, $^1J_{\text{Pt-P}} = 3324$ Hz), -30.3 (d, $^2J_{\text{P-P}} = 23.8$ Hz, ^{195}Pt satellites, $^1J_{\text{Pt-P}} = 3496$ Hz). Anal. Calcd for $\text{C}_{160}\text{H}_{212}\text{F}_{48}\text{N}_{16}\text{O}_{16}\text{P}_{24}\text{Pt}_8$: C, 32.95; H, 3.66; N, 3.84. Found: C, 33.16; H, 3.60; N, 3.74.

Acknowledgment. P.J.S. thanks the NIH (Grant GM-057052) for financial support.

Supporting Information Available: Detailed characterization of assemblies **4**, **7–12**, and **14**, general procedure for the supramolecular transformation experiments, and details of the computational study. This material is available free of charge via the Internet at <http://pubs.acs.org>.

JA106251F